Needleless Electrospinning Using a Flat Wheel Spinneret

Usman Ali, PhD, Amir Abbass, PhD, Furqan Khurshid, PhD, Sarmad Aslam, PhD, Abdul Waqar, PhD

Bahauddin Zakariya University, Textile Engineering, Multan, Punjab PAKISTAN

Correspondence to:
Usman Ali email: usman.ali@bzu.edu.pk

ABSTRACT

Nanofibers have a wide range of applications, however; the mass production of nanofibers is still an obstacle to wider industrial application. In this paper, a flat wheel was used as a spinneret for production of poly (vinyl) alcohol nanofibers. Electric field comparative analysis was done between the flat wheel and other spinnerets such as a cylinder, disk and ring. It was found the flat wheel falls between the cylinder and disk and ring spinnerets. Sequence generation of polymer jets was observed from the both edges of the wheel and as well as from the surface of the wheel. The impact of operating parameters on fiber morphology was studied and it was found that smooth, uniform nanofibers with diameter around 350nm could be produced by using this spinneret. Influence of strength of applied electric field and solution concentration on the production rate was also examined and it was noted that the production rate of nanofibers using a flat wheel spinneret is several times higher than that obtained using a conventional needle electrospinning setup.

Keywords: Nanomaterials**,** Needleless electrospinning, Flat wheel, Production

INTRODUCTION

The production of nanofibers has gained the attention of scientists from all over the world in the last decades [1, 2]. Electrospinning is a well-known technique for producing nanofibers from different materials, Nanofiber production techniques include self-assembly [3], drawing [4], phase-separation and template synthesis. Electrospun nanofibers are used in applications in such as micro manufacturing engineering, energy storage as well as medical and protective clothing [5-8]. The production rate of the basic electrospinning setup is very low (around 300 mg per hour [9]) which makes industrial scale implementation impractical.

Inventors have shown considerable interest in increasing the productivity of electrospun nanofibers, investigating such techniques as creating multiple jets From a single needle either by using a curved collector [10], by using a needle with a grooved tip [11] and by using an air jacket to improve the fiber production process [12, 13]. Dosunmu et al. [14] investigated multiple jet formation from a cylindrical tube. Varabhas et al. [15] modified their setup with linear hole array arrangements. Multi-needle electrospinning is a straight-forward method used to increase the electrospinning productivity. Different attempts have been made to increase production by placing the needles linear, concentric array, elliptic and hexagonal arrays [16-18]. Problems associated with multi-needle arrays include nozzle blockage, large operating space requirements and optimization of needle locations in order to avoid unevenly deposited nanofiber mats.

Jets can also be generated from the free surface of a liquid in a process known needleless electrospinning. In needleless electrospinning, a spinneret is placed in the solution bath and a high strength electric field is applied to the solution bath and collector. This results in the formation of numerous jets from the spinneret and the nanofibers form on a collector. In 2005 Jirsk et al. [19] patented a needleless electrospinning mechanism using a roller or cylinder as a fiber spinneret. This has been commercialized by Elmarco with the brand name Nanospider. The shape and geometry of the spinneret play a vital role in the generation of polymer jets. Recently efforts have been made to optimize the shape of spinneret to increase the production and quality of nanofibers. Examples include the use of edge plate geometry [20], conical wire coil [9], charge rotating cone [21], disk [22], flat spinneret [23], umbellate nozzles [24], wire electrode [25-28], porous material [29], pyramid [30, 31], high pressure spray gun [32], foam spinning [33], vertical rod [34, 35] and spiral coil spinneret [36-38]. Attempts have also been made to modify the surface of the spinneret by using a tipped surface (Hunag et al. 2007) . Lin's team studied [39] the electric field profile in the electrospinning zone and compared the electrical field intensity profile of cylinder, disc and coil. They noted that the intensity

of the electric field profile is the main driving force in initiating the jets. They also noted that the electric field in the cylinder was mainly located around the edges of the cylinder, whereas in the coil the electric field is smoothly distributed along the whole coil, resulting in higher nanofiber production rates. Nevertheless, more efficient spinneret geometries having the capabilities of higher uniform electric field distribution and high quality fiber morphology are still in demand. In this work, a flat wheel is used as a spinneret to electrospin poly (vinyl) alcohol (PVA) nanofibers. Higher intensity of electrical field on the edges of the wheels was observed, resulting in higher productivity of fibers with finer diameters. The effect of the different experimental parameters on fiber morphology and productivity were studied in detail.

MATERIALS AND METHODS

Materials

Polyvinyl alcohol (PVA) with an average molecular weight of 146,000-186,000 and hydrolyzed 96% was purchased from sigma-Aldrich, USA and used as received. Polyvinyl alcohol solutions of 7, 8, 9 and 10 wt% concentrations were prepared by dissolving PVA powder in distilled water and stirring continuously for 24hrs at 80ºC. The solution properties such as surface tension and conductivity were measured by using stalagmometer and conductivity meter respectively.

Needleless Electrospinning Setup

Figure 1 depicts schematically the apparatus used in this study for needleless electrospinning. It consists of a flat wheel, solution bath, rotating collector covered with aluminum foil and a high voltage power supply (ES100P, Gamma High Voltage Research). The rotating flat-wheel was used as a spinneret to raise polymer solution from the reservoir. It is 150 mm in diameter, 25mm wide, 2mm thick.

An electrode was inserted into the solution reservoir to connect to the polymer solution to a high voltage power supply. A rotating drum covered with aluminum foil was used to collect the nanofibers [40]. The speed of drum was set at 150 rpm for all the experiments. All experiments were conducted under standard atmospheric conditions, i.e. temperature 20 ± 5ºC and relative humidity 65 ± 5%.

Determination of Electric Field Profile,

Electric field simulation was done using the software COMSOL Multiphysics 5.0.

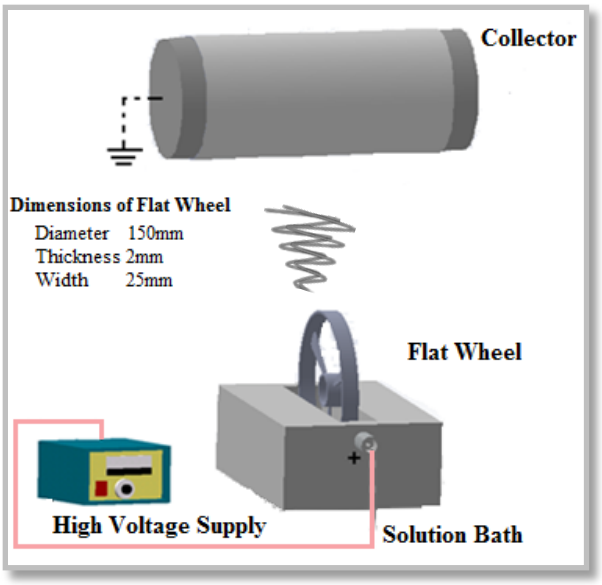

FIGURE 1. Schematic illustration of the Flat Wheel Needleless Electrospinning setup.

Determination of Surface Morphology and means fiber diameter

The fiber morphology was observed under a scanning electron microscope (Neoscope). The mean fiber diameter was measured from the SEM images using an image-analysis software (Image*Pro*+6.0). One hundred measurements were taken from at least ten SEM images selected randomly from different areas of each sample.

Determination of Productivity of Nanofibers

The production rate of fibers was determined by running the setup continuously for 60 minutes for each parameter. Five measurements were taken for each sample. The weights of electrospun nonwoven matts were determined with an analytical balance (Excellence XS).

RESULTS AND DISCUSSION

Design for Needleless Electrospinning Setup

The designed needleless electrospinning setup and the images of the ongoing process are shown in *Figure 1* and *Figure 2*(*a-b*) respectively. As illustrated in *Figure 1* the flat wheel spinneret was used as a generator to produce polymeric nanofibers. The spinneret was dipped approximately one-fifth in the solution reservoir and was rotated using a 12v DC motor. Due to the rotation of spinneret and viscoelastic nature of polymer solution a thin layer of polymer solution was formed on the surface of the

flat wheel and around its smooth edges. When the flat wheel with a thin layer of the solution was charged with strength of applied electric field around 45KV, polymer jets start generating from the upper surface of the flat wheel. Further increasing the strength of applied electric field to 60KV resulted in generation of several polymer jets emerging from the edge of the spinneret and the surface between the edges as shown in *Figure 2a-b*. It was noted that the thickness of solution layer on the wheel was affected by rotation speed and the jet formation area and fiber production were disturbed. When the rotation speed of the wheel was less than 5 rpm a very fine layer of solution was formed on the wheel and thus the fiber formation occurred earlier, resulting in low production of fibers When rotation speed of the wheel was greater than 8 rpm a thick layer was formed, resulting in later formation of fibers, low production and coarser fibers. It was found the wheel has the optimum fiber formation when its rotation speed is between 5-8 rpm. It was also observed that more jets were produced from the edges as compared to the middle surface area. This was most likely due to the distribution of electric field which made the electrical force stronger at the edges as compared to the middle surface area as shown in *Figure 2c*. *Figure 2d* shows the proposed spiral flat wheel spinneret for industrial use.

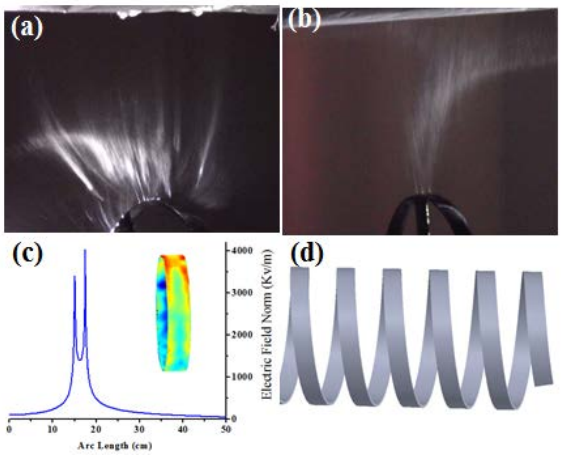

FIGURE 2. a-b) Showing photographs of ongoing Flat wheel needleless electrospinning process at different angles showing the formation of jets, c) Electric field profile and electric field norm on the Flat wheel spinneret and d) Schematic diagrams of proposed spinneret.

A comparison was made between the flat wheel and other commonly used spinnerets such as cylinder and disk and ring by measuring the electric field intensities, also known as the electric field norm. This may be defined as the strength of applied electric field on a particular point of the spinneret placed in an electric field. It was measured by drawing an imaginary line on the upper surface of the spinneret known as arc length. The dimensions of these spinnerets are: cylinder; length = 200 mm diameter = 150 mm, disk and ring both having thickness = 3 mm and diameter = 150 mm. These shapes were made in solid works and electric field profile and electric field norms were measured by using software COMSOL Multiphysics 5.0. *Table I* shows the electric field profile of the cylinder, flat wheel and disk and ring. The graphical comparison of the electric field norm of the cylinder, flat wheel and disk and ring is shown in *Figure 3*. From this graph, it can clearly be seen that the electric field profile for the flat wheel is similar to the cylinder but with higher electric field norm on the edges of 3500 KV/m as compared to the cylinder, which has an electric field norm on the edges around 2400 KV/m. Further, the intensity of electric field profile at the middle area of the flat wheel is also higher at 1300 KV/m as compared to the middle area of a cylinder, which has an intensity of around 800 KV/m.

Since the flat wheel has much higher electric field intensity on both edges and middle area than the cylinder, more jets will be produced from the flat wheel than the cylinder. On the other hand, the electric field intensity on the flat wheel (3500 KV/m) is almost half of the electric field intensity than the ring and disk (6500 KV/m). Based on the above analysis it can be said that flat wheel is an intermediate spinneret that has electric field intensity higher than the cylinder but lower than the ring and disk, may be scaled up like a spiral coil and will generate two peaks instead of one as in the case of the ring and disk.

TABLE I. Showing the Electric Field Profile on the Cylinder, Flat Wheel, Disk and Ring.

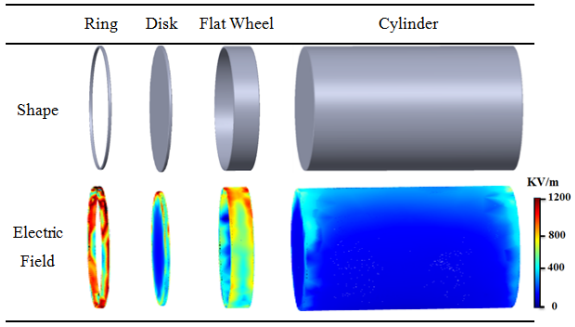

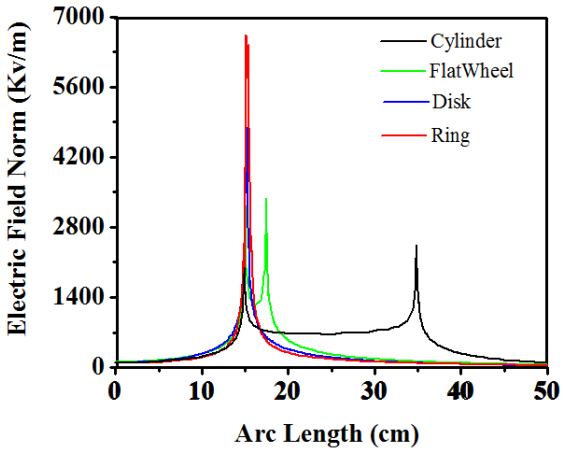

FIGURE 3. Graphical comparison of the electric field norm on the cylinder, Flat Wheel, Disk and Ring under the applied electric field strength of 65KV.

Influence of Operating Parameters on Mean Fiber Diameter

Applied Electric Field Strength

Applied electric field strength, also known as applied voltage plays a key role during the formation of nanofibers in electrospinning. In this study, a series of experiments were conducted to observe the influence of applied electric field strength on the fiber diameter and diameter distribution of the fibers produced by using this spinneret. Strength of applied electric field was increased from 45 KV to 75 KV by keeping the polymer solution concentration and collecting distance constant (i.e. 8 wt% and 13 cm respectively). *Figure 4* shows the histograms of fiber diameter distributions with different electric field strengths.

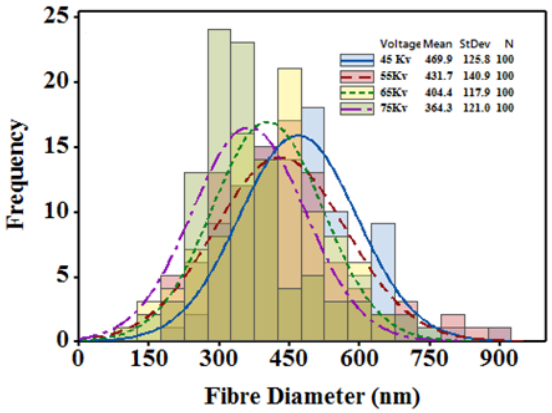

FIGURE 4:- Shows the Histogram of individual fibers diameter under the influence of applied electric field strength, whereas solution concentration 8wt% and spinning distance 13cm were kept constant.

The distribution curves of 45 KV and 55 KV show a main peak at about 450 nm and the peaks of the 65 KV and 75KV curves were around 350nm. This is possibly due to the higher strength of the electric field, resulting in higher jet extension. It can be seen that there is a dramatic decrease in fiber diameter as the strength of applied electric field is increased. With the increase in strength of applied electric field from 45 KV to 75 KV, the mean diameter of nanofibers decreases from 469.87±125.80 nm to 364.33±121.02 nm. It can be seen that the diameter of 80-90% of the fibers lies in the range of 150 nm to 600 nm.

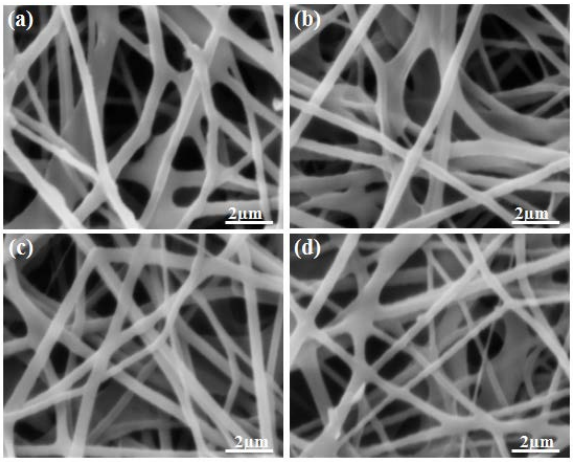

FIGURE 5. SEM Photos of electrospin nanofibers (with magnification 10000 times) at different strength of applied electric field: a) 45KV, b) 55KV, c) 65KV and d) 75KV respectively, whereas solution concentration 8wt% and spinning distance 13cm were kept constant.

Figure 5 shows the effect of applied electric field strength on the surface morphology of the needleless electrospun PVA nanofibers. It can be seen clearly from these SEM images that under low strength of applied electric field at 45 KV and 5 5KV, the morphology of some fibers is branch shaped. Further, some of the fibers are found to be one micron or even higher in diameter as shown in *Figure 5a* and *5b*. When the strength of the applied electric field increases to 6 5KV, the fibers become fine and even, the branch shaped fibers disappear. When the strength of applied electric field increases to75 KV, the diameter of most of the fibers decreased to around 350 nm, with some fibers having diameters as low as 150 nm, as shown in *Figure 5d*.

Solution Concentration

To determine the influence of polymer solution concentration on the spinning process, PVA solutions of different concentrations were prepared and needleless spinning was carried out. *Figure 6* shows the effect of PVA concentration on mean fiber diameter with standard deviations. It is evident from the *Figure 6* that an increase in the concentration of PVA from 7 wt% to 10 wt% results in the increase in mean diameter from 431 nm to 557 nm. This is because the increase in the concentration of PVA solution results in increase of solution viscosity, surface tension and conductivity. Hence, the cohesive forces among the molecules become stronger. Due to these strong, cohesive forces, there was less drawing of the polymer solution as a result of the whipping motions of the jets. This lack of polymer drawing consequently results in the production of fibers of higher diameter.

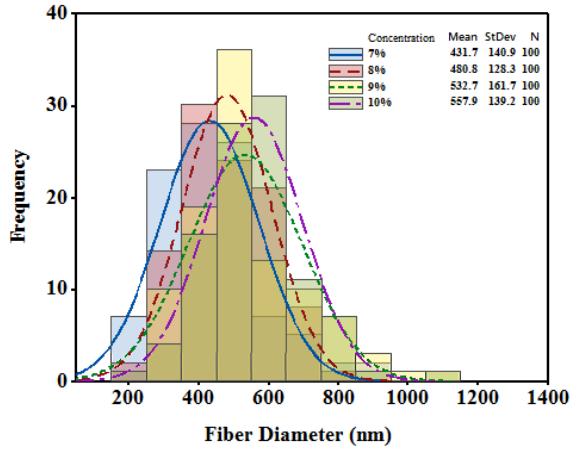

FIGURE 6. Shows the Histograms of individual fiber diameter under the influence of concentration, whereas strength of applied electric field 55KV and spinning distance 13cm were kept constant.

The solution with ta concentration of 7 wt% (surface tension 75.63 dynes per centimeter; conductivity 682 Siemens) and 8 wt% (surface tension 80.33 dynes per centimeter; conductivity 746 Siemens) produced the majority of fibers with a diameter in the range of 400 nm to 50 nm, and all the fibers produced were under 1-micron. When the concentration was raised to 9 wt% (surface tension 86.02 dynes per centimeter; conductivity 796 Siemen's) and 10 wt% (surface tension 91.14 dynes per centimeter; conductivity 835 Siemens) a much wider range of fiber diameter distributions was observed.

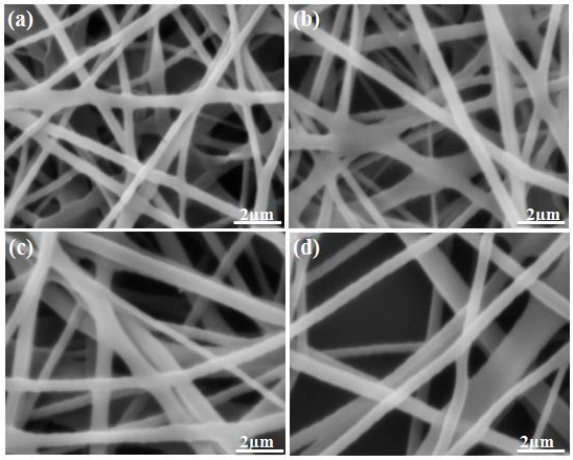

FIGURE 7. SEM Photos of electrospin nanofibers (magnification 10000 times) with different PVA concentrations: a) 7 wt%, b) 8 wt%, c) 9 wt% and d) 10 wt%, respectively, whereas strength of applied electric field 55 KV and spinning distance 1 3cm were kept constant.

Figure 7 shows the effect of PVA concentration on the surface morphology of the needleless electrospun PVA nanofibers. It is evident from these SEM images that all PVA fibers have a diameter less than 1.2 microns. As shown in *Figure 7a and 7b*, the PVA concentration of 7 wt% and 8 wt% produced fibers of less than 0.9 micron diameter. It can also be seen that these samples have very tiny small fibers with a diameter around 200nm. When the concentration was raised to 9 wt% and 10 wt%, these tiny fibers disappear and many coarse fibers were produced. Some such fibers have diameters greater than one micron, as shown in photo *Figure 7c and 7d* respectively This results in an increase of mean fiber diameter and an increase in standard deviation.

Collecting Distance

The distance between the spinneret and the collector was changed to determine the influence on the fiber morphology and diameter. The collecting distance was changed from 10cm to 16cm while keeping all the other experimental parameter constant, including

strength of applied electric field 55 KV and polymer solution concentration 8 wt%. *Figure 8* shows the diameter analysis of fibers produced by varying the collecting distance.

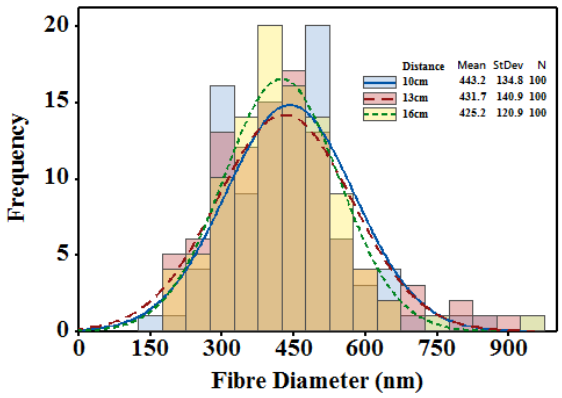

FIGURE 8. Shows the Histogram of individual fiber diameter under the influence of spinning distance, whereas solution concentration 8wt% and strength of applied electric field 55KV were kept constant

When the collecting distance was varied from 10 cm to 16cm, nanofiber diameters decrease from 443 nm to 425 nm as do the standard deviations from 134 nm to 120nm respectively. When the distance is too short, the jets could not be drawn sufficiently during the whipping process. Due to this lack of drawing effect, the resulting fibers diameters are coarser with wider deviation. Increasing the distance increases the time available for stretching the stretching in the whipping process, resulting in finer fibers with lower deviation. The distribution of fibers with collecting distances 10 cm and 13 cm looks similar, with the main peak around 450 nm. The main peak of nanofibers with a collecting distance of 16 cm is around 400 nm. From *Figure 8* it is also noted that the differences in fiber diameter obtained at different collecting distance are not statistically significant. This is because when distance is decreased the fiber flight path is reduced This favors the formation of coarser fibers However, reduction in the collecting distance results in higher electric field intensity on the spinneret which favors the formation of finer fiber When the collecting distance is increased, these competing effects on fiber size occur in reverse. *Figure 9* shows the surface morphology of PVA nanofibers produced under varied collecting distances. From these photos, it can be seen clearly that all the fibers are very fine with a diameter much lower than 750 nm, with only a few fibers having a diameter around 1 micron, as shown in *Figure 9a*.

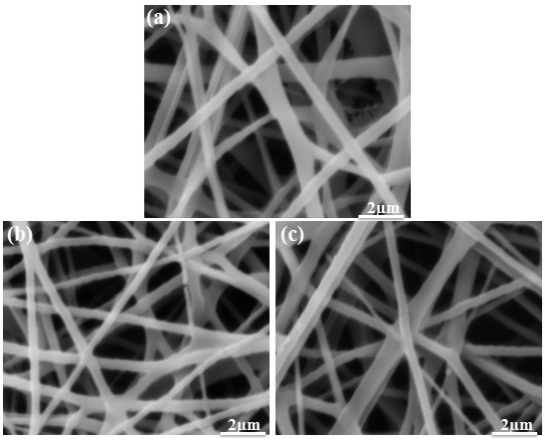

FIGURE 9. SEM Photos of electrospin nanofibers (with magnification 10000 times) at different collecting distances: a) 10cm, b) 13cm and c) 16cm respectively, whereas solution concentration 8wt% and strength of applied electric field 55KV were kept constant.

Fiber Productivity

In needleless electrospinning, the productivity of fibers depends upon the concentration of polymer solution and the strength of the applied electric field on the surface of the spinneret. *Figure 10* shows the productivity of nanofibers produced by using this novel spinneret. It shows the effect of polymer solution concentration and strength of applied electric field on the productivity of nanofibers keeping the experimental parameters constant as follows: rotating speed between 5-8 rpm and spinning distance 13 cm. It was found that an increase in strength of the applied electric field resulted in a direct increase in fiber productivity. This is because an increase in the strength of applied electric field results in an increase in the electric field intensity at the surface of spinnerets causes the development of multiple jets which results in higher production. Nevertheless, it was also noted that when the strength of applied electric field was very low (less than 45KV) the drawing strength was insufficient to produce continuous jets from the surface of the spinneret and the spinning was not continuous. At a given strength of applied electric field and spinning distance it was noted that by varying the polymer solution concentration the fiber productivity first increases and then it decreases. This may be due to increasing in viscosity of polymer solution and resulting decrease in draw ability.

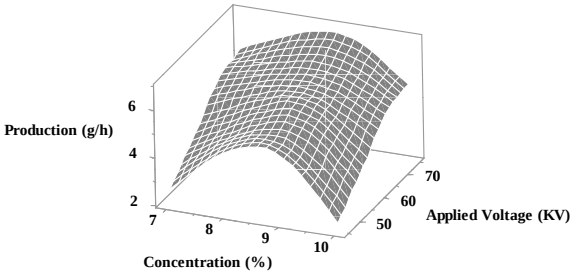

FIGURE 10. Productivity of Flat Wheel Needleless Electrospinning setup at different solution concentrations and strength of applied electric field whereas spinning distance 13cm was kept constant.

A comparison of production rate of the flat wheel spinneret with alternate needleless electrospinning spinnerets such as the cylinder and disk and ring was also made. *Figure 11* shows the effect of applied electric field strength on production of different spinnerets, with polymer solution concentration and collection distance constant. It was found that the production of all the spinnerets increased with the increase in the strength of applied electric field; however, the production of flat wheel is higher than the cylinder spinneret but lower than that of the disk and ring spinnerets.

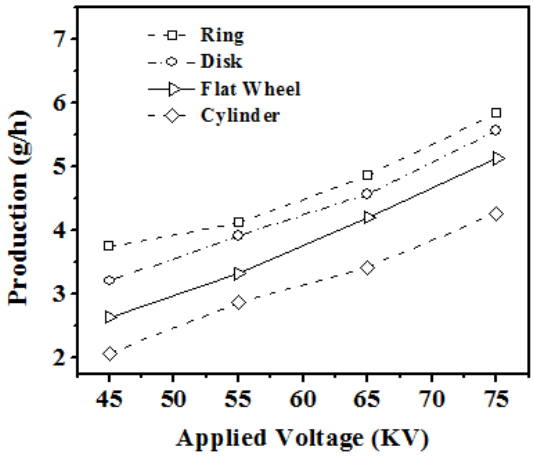

FIGURE 11. Shows the production of different spinnerets under the effect of applied electric field strength, whereas solution concentration 8wt% and spinning distance 13cm were kept constant.

CONCLUSION

This work demonstrates the needleless electrospinning of PVA nanofibers by using a flat wheel spinneret. A series of polymer jets was produced from the wheel surface and also from the edges of the flat wheel. Influence of operating parameters such as strength of applied electric field, polymer solution concentration and collecting distance on mean fiber diameter, diameter distribution and fiber productivity was studied. It was found that the mean fiber diameter, diameter distribution and fiber productivity could be controlled by varying these parameters. The productivity of this spinneret was 15-40 times higher than that of the conventional needle electrospinning mechanism and much closer to the ring and disk. The results revealed that this spinneret could be further developed into a "middle-class" electrospinning system for the mass production of nanofibers at industrial scale.

ACKNOWLEDGEMENT

This research was funded by Bahauddin Zakariya University, College of Textile Engineering, Multan. The authors also acknowledge Deakin University for helping with characterization to complete this research project.

REFERENCES

[1] Bhardwaj, N. and S.C. Kundu, *Electrospinning: A fascinating fiber fabrication technique.* Biotechnology Advances, 2010. 28(3): p. 325-347.

[2] Haider, A., S. Haider, and I.-K. Kang, *Comprehensive review summarizing effect of electrospinning parameters and potential applications of nanofibers in biomedical and biotechnology.* Arabian Journal of Chemistry.

[3] Rolandi, M. and R. Rolandi, *Self-assembled chitin nanofibers and applications.* Advances in Colloid and Interface Science, 2014. 207: p. 216-222.

[4] Bajáková, J., J. Chaloupek, D. Lukáš, And M. Lacarin, *Drawing" The Production Of In Divdual Nanofibers By Experimental Method.* Nanocon, 2011. 9: P. 21-23.

[5] Zhang, B., F. Kang, J.-M. Tarascon, and J.-K. Kim, *Recent advances in electrospun carbon nanofibers and their application in electrochemical energy storage.* Progress in Materials Science, 2016. 76: p. 319-380.

[6] Ramakrishna, S., K. Fujihara, W.-E. Teo, T. Yong, Z. Ma, and R. Ramaseshan, *Electrospun nanofibers: solving global issues.* Materials Today, 2006. 9(3): p. 40-50.

[7] Chen, G., J. Guo, J. Nie, and G. Ma, *Preparation, characterization, and application of PEO/HA core shell nanofibers based on electric field induced phase separation during electrospinning.* Polymer.

[8] Chronakis, I.S., *Chapter 22 - Micro- and Nano-fibers by Electrospinning Technology: Processing, Properties, and Applications*, in *Micromanufacturing Engineering and Technology (Second Edition)*, Y. Qin, Editor. 2015, William Andrew Publishing: Boston. p. 513-548.

[9] Wang, X., H. Niu, T. Lin, and X. Wang, *Needleless electrospinning of nanofibers with a conical wire coil.* Polymer Engineering & Science, 2009. 49(8): p. 1582-1586.

[10] Vaseashta, A., *Controlled formation of multiple Taylor cones in electrospinning process.* Applied Physics Letters, 2007. 90(9): p. 093115.

[11] Yamashita, Y., F. Ko, A. Tanaka, and H. Miyake, *Characteristics of Elastomeric Nanofiber Membranes Produced by Electrospinning*. Journal of Textile Engineering, 2007. 53(4): p. 137-142.

[12] Li, L., W. Kang, X. Zhuang, J. Shi, Y. Zhao, and B. Cheng, *A comparative study of alumina fibers prepared by electro-blown spinning (EBS) and solution blowing spinning (SBS).* Materials Letters, 2015. 160: p. 533-536.

[13] Zhao, Y.-X., X.-H. Zhou, L. Li, W. Xu, W.-M. Kang, and B.-W. Cheng, *Preparation of porous CeO2/CuO/Al2O3 fibers via electro-blown spinning method.* Materials Letters, 2016. 164: p. 460-463.

[14] Dosunmu, O.O., G.G. Chase, W. Kataphinan, and D.H. Reneker, *Electrospinning of polymer nanofibres from multiple jets on a porous tubular surface.* Nanotechnology, 2006. 17(4): p. 1123-7.

[15] Varabhas, J.S., G.G. Chase, and D.H. Reneker, *Electrospun nanofibers from a porous hollow tube.* Polymer, 2008. 49(19): p. 4226-4229.

[16] Kim, G., Y.-S. Cho, and W.D. Kim, *Stability analysis for multi-jets electrospinning process modified with a cylindrical electrode.* European Polymer Journal, 2006. 42(9): p. 2031-2038.

[17] Theron, S.A., A.L. Yarin, E. Zussman, and E. Kroll, *Multiple jets in electrospinning: experiment and modeling.* Polymer, 2005. 46(9): p. 2889-2899.

[18] Varesano, A., R.A. Carletto, and G. Mazzuchetti, *Experimental investigations on the multi-jet electrospinning process.* Journal of Materials Processing Technology, 2009. 209(11): p. 5178-5185.

[19] O. Jirsak, F. Sanetrnik, D. Lukas, V. Kotek, L. Martinova, and J. Chaloupek. *A method of nanofibres production from a polymer solution using electrostatic spinning and a device for carrying out the method*. "WO 2005/024101 A1, 2005".

[20] Thoppey, N.M., J.R. Bochinski, L.I. Clarke, and R.E. Gorga, *Unconfined fluid electrospun into high quality nanofibers from a plate edge.* Polymer, 2010. 51(21): p. 4928-4936.

[21] Lu, B., Y. Wang, Y. Liu, H. Duan, J. Zhou, Z. Zhang, Y. Wang, X. Li, W. Wang, W. Lan, and E. Xie, *Superhigh-Throughput Needleless Electrospinning Using a Rotary Cone as Spinneret.* Small, 2010. 6(15): p. 1612-1616.

[22] Li, D., T. Wu, N. He, J. Wang, W. Chen, L. He, C. Huang, H.A. Ei-Hamshary, S.S. Al-Deyab, Q. Ke, and X. Mo, *Three-dimensional polycaprolactone scaffold via needleless electrospinning promotes cell proliferation and infiltration.* Colloids and Surfaces B: Biointerfaces, 2014. 121(0): p. 432-443.

[23] Zhou, F.-L., R.-H. Gong, and I. Porat, *Polymeric nanofibers via flat spinneret electrospinning.* Polymer Engineering & Science, 2009. 49(12): p. 2475-2481.

[24] Li, H., H. Chen, X. Zhong, W. Wu, Y. Ding, and W. Yang, *Interjet distance in needleless melt differential electrospinning with umbellate nozzles.* Journal of Applied Polymer Science, 2014. 131(15): p. n/a-n/a.

[25] Forward, K.M. and G.C. Rutledge, *Free surface electrospinning from a wire electrode.* Chemical Engineering Journal, 2012. 183(0): p. 492-503.

[26] Jani, H., P. Toni, S. Eero, and R. Mikko, *Needleless electrospinning with twisted wire spinneret.* Nanotechnology, 2015. 26(2): p. 025301.

[27] Liu, Y., L. Zhang, X.-F. Sun, J. Liu, J. Fan, and D.-W. Huang, *Multi-jet electrospinning via auxiliary electrode.* Materials Letters, 2015. 141: p. 153-156.

[28] Bhattacharyya, I., M.C. Molaro, R.D. Braatz, and G.C. Rutledge, *Free surface electrospinning of aqueous polymer solutions from a wire electrode.* Chemical Engineering Journal, 2016. 289: p. 203-211.

[29] Jiang, G., S. Zhang, and X. Qin, *High throughput of quality nanofibers via one stepped pyramid-shaped spinneret.* Materials Letters, 2013. 106(0): p. 56-58.

[30] Jiang, G. and X. Qin, *An improved free surface electrospinning for high throughput manufacturing of core–shell nanofibers.* Materials Letters, 2014. 128(0): p. 259-262.
[31] Jiang, G., S. Zhang, and X. Qin, *Effect of processing parameters on free surface electrospinning from a stepped pyramid stage.* Journal of Industrial Textiles, 2014.
[32] He, J., Y. Lian, X. Zhang, Y. Wu, and R. Liu, *Mass preparation of nanofibers by high pressure air-jet split electrospinning: Effect of electric field.* Journal of Polymer Science Part B: Polymer Physics, 2014. 52(15): p. 993-1001.
[33] Higham, A.K., C. Tang, A.M. Landry, M.C. Pridgeon, E.M. Lee, A.L. Andrady, and S.A. Khan, *Foam electrospinning: A multiple jet, needle-less process for nanofiber production.* AIChE Journal, 2014. 60(4): p. 1355-1364.
[34] Shin, H.U., Y. Li, A. Paynter, K. Nartetamrongsutt, and G.G. Chase, *Vertical rod method for electrospinning polymer fibers.* Polymer, 2015. 65: p. 26-33.
[35] Shin, H.U., Y. Li, A. Paynter, K. Nartetamrongsutt, and G.G. Chase, *Microscopy analysis and production rate data for needleless vertical rods electrospinning parameters.* Data in Brief, 2015. 5: p. 41-44.
[36] Zhou, Z., X.-F. Wu, Y. Ding, M. Yu, Y. Zhao, L. Jiang, C. Xuan, and C. Sun, *Needleless emulsion electrospinning for scalable fabrication of core–shell nanofibers.* Journal of Applied Polymer Science, 2014. 131(20): p. n/a-n/a.
[37] Wang, X., T. Lin, and X. Wang, *Scaling up the production rate of nanofibers by needleless electrospinning from multiple ring.* Fibers and Polymers, 2014. 15(5): p. 961-965.
[38] Wang, X., X. Wang, and T. Lin, *Electric field analysis of spinneret design for needleless electrospinning of nanofibers.* Journal of Materials Research, 2012. 27(23): p. 3013-3019.
[39] Niu, H., T. Lin, and X. Wang, *Needleless electrospinning. I. A comparison of cylinder and disk nozzles.* Journal of Applied Polymer Science, 2009. 114(6): p. 3524-3530.
[40] Katta, P., M. Alessandro, R.D. Ramsier, and G.G. Chase, *Continuous Electrospinning of Aligned Polymer Nanofibers onto a Wire Drum Collector.* Nano Letters, 2004. 4(11): p. 2215-2218.

AUTHORS' ADDRESSES

Usman Ali, PhD
Amir Abbass, PhD
Furqan Khurshid, PhD
Sarmad Aslam, PhD
Abdul Waqar, PhD
Bahauddin Zakariya University
Textile Engineering
6Km Khanewal Road
Multan, Punjab 59060
PAKISTAN